Supplemental Figure Legend

Figure S1. Additional Evidence Supporting the Recruitment of mRNPs to MOM and Role of MOM-Associated mRNPs in Recruiting Autophagy Receptors to Damaged Mitochondria, Related to Figure 1

(A) Immunoblots showing lack of enhanced recruitment of autophagy receptors to mitochondria in CCCP (20 μM) treated *PINK1(-/-)* HeLa cells.

(B) Immunoblots assessing the extent of ER contamination in crude (c) and Percoll gradient-purified (p) mitochondria.

(C) Additional immunoblots showing the release of various factors by RNase A or EDTA treatment of mitochondrial fractions from HeLa or HeLa/GFP-Parkin cells. Immunoblots of mitochondrial pellets (pel) and released fractions (sup) are shown. * marks a presumably ubiquitinated form of Tom20 seen in HeLa/GFP-Parkin but not HeLa cells.

(D) TMRM staining showing loss of mitochondrial membrane potential (MMP) after treatment of HeLa cells with 20 μM CCCP, and recovery of MMP after washout of CCCP.

(E) ATP measurement showing reduction of ATP level after 2hr of 20 μM CCCP treatment of HeLa cells, and recovery after washout of CCCP. ** and ## indicate $p<0.005$ in Student's *t*-tests.

(F, G) Propidium Iodide (PI) staining showing lack of cell death in HeLa cells treated with CCCP for 2hrs or 6 hrs. F shows data quantification. ** indicates $p<0.005$ in *Chi-squared* test. Positive control represents cells directly fixed with formaldehyde and then stained with PI. More than 500 cells were counted in each group.

(H) ATP measurement of HeLa cells treated with 20 μM CCCP for the indicated times. Relative ATP levels normalized to time 0 are used in statistical analysis. * indicates $p<0.05$ in Student's *t*-test.

(I) Immunoblots detecting levels of actin and C-I30 proteins in HeLa cells treated with graded concentrations of CCCP for the indicated periods.

(J) Immunoblots of mitochondrial fractions from HeLa or HeLa/GFP-Parkin cells treated with 10 μM Antimycin A and 10 μM Oligomycin (A/O) for the indicated duration, showing recruitment of co-translational quality control factors and autophagy receptors to mitochondria and mitochondria-associated *C-I30* mRNPs. Ubiquinol-cytochrome c reductase complex core protein 2 (Core 2) serves as mitochondrial loading control.

Figure S2. Additional Evidence Supporting that Mitochondrial Damage Causes Accumulation of Co-Translational Quality Control Factors to Translationally Stalled Ribosome/mRNPs on MOM, Related to Figure 2

(A) Immunoblots of C-I30 mRNP purified from mitochondria of *PINK1(-/-)* HeLa cells showing the lack of recruitment of autophagy receptors in response to CCCP treatment.

(B) RT-PCR analysis showing the extent of MS2-bs-tagged C-I30 mRNA overexpression in HeLa cells used for the MS2-bs/MS2-GST tagging analysis. Primer pair 1 amplifies only MS2-bs-tagged *C-I30* mRNA, whereas primer pair 2 amplifies both endogenous and transfected *C-I30* mRNA. Left lane: non-transfected cells. Right lane: HeLa cells transfected with MS2-bs-tagged *C-I30* cDNA.

(C) Immunoblots of C-I30 mRNP purified from mitochondria of HEK293T cells transfected with PINK1-WT or pathogenic PINK1-G309D.

(D) RT-PCR analysis of *C-I 30* mRNA level on MOM in various HeLa cell lines upon CCCP treatment, with mitochondrially-encoded *C-IV s.1* as loading control. RT-PCR shows quality of the mitochondrial preparation. *, $p<0.05$ in Student's *t*-test.

(E) RT-PCR analysis showing the enrichment of *PINK1* mRNA, and PINK1-dependent enrichment of *nRCC* mRNAs on MOM of rotenone-treated fly muscle.

(F) RT-PCR analysis showing enhanced recruitment of *C-I30* mRNA to MOM of HeLa cells treated with rotenone (Rtn) but not H_2O_2.

(G) RT-PCR analysis showing lack of enhanced recruitment of *C-I30* mRNA to MOM of HeLa cells overexpressing the deletion mutant of OTC (ΔOTC) that is known to accumulate in the mitochondrial matrix and induce mitochondrial unfolded protein response in mammalian cells. Note that ΔOTC did induce mitochondrial damage and cause PINK1 stabilization.

(H) Puromycin labeling of newly synthesized NPCs in purified mitochondria fractions treated with Chloramphenicol (CAP) or RNase A. The abolishment of puromycin incorporation by RNase A treatment, which degrades MOM-associated mRNAs, but not CAP, which specifically inhibits translation by mitochondrial ribosomes, supports the notion that puromycin primarily labels MOM-associated cytosolic mRNP/ribosomes, not matrix-localized mitochondrial ribosomes. Core 2 and Actin were used as the mitochondrial and cytosolic markers, respectively, to verify the purity of the samples.

(I) Immunoblots showing increased signals of primarily K48-linked poly-ubiquitin, in the newly synthesized NPCs on MOM upon CCCP treatment. Newly synthesized NPCs were labeled with puromycin, immunoprecipitated with anti-Puromycin antibody, and probed with chain-specific anti-Ub antibodies.

Figure S3. Additional Analysis of Co-Translational Quality Control Factors and Their Interactions, Related to Figure 3

(A) Immunoblots of mitochondrial fractions from HeLa cells treated with low concentration (5 μM) CCCP, showing recruitment of co-translational quality control factors to mitochondria and mitochondria-associated *C-I30* mRNPs.

(B) RNA-IP showing association of *C-I30* mRNA with endogenous ABCE1, Pelo, and NOT4, and enhanced association of *C-I30* mRNA with ABCE1 and NOT4 upon CCCP treatment.

(C) PLA assay showing enhanced interaction between ABCE1 and C-I30 mRNP on mitochondria upon CCCP treatment. Arrowheads indicate cytoplasmic (white) and mitochondrial (yellow) co-localization.

(D) Evidence of ribosome splitting on MOM in CCCP treated HeLa cells. Immunoblots show distinct behavior of small (S) and large (L) ribosomal subunits. Diagram depicts a plausible scenario of their differential distribution. The L subunit is possibly anchored to MOM through NPCs in transit through the TOM/TIM import complex.

(E) Immunoblots showing increased recruitment of ABCE1 and Pelo to Percoll-purified damaged mitochondria of *dPINK1* mutant muscle. The blot on the right shows specificity of the anti-dPelo antibody.

(F) Immunostaining showing enhanced recruitment of Pelo and ABCE1 to abnormal mitochondria in *Mhc>PINK1 RNAi* muscle. A HA-tagged *dABCE1* transgene was used to monitor ABCE1 localization.

(G) Immunoblots showing the release of co-translational quality control factors by RNase A and EDTA treatments of mitochondria from HeLa or HeLa/GFP-Parkin cells.

(H) Immunoblots showing effect of pathogenic PINK1-G309D on the recruitment of ABCE1, Pelo, and NOT4 to C-I30 mRNP purified from HEK293 cells.

(I) Co-IP assays showing the interaction between Pelo and PINK1 in fly muscle tissue.

(J) Co-IP assays showing the interaction of Pelo, ABCE1, and NOT4 with PINK1 in HeLa cells.

(K) Immunoblots showing the protein levels of NOT4 and Pelo in NOT4 strong (S), medium (m), or weak (w) overexpression (OE) fly lines. CI-75 was used as the loading control.

(L) Western blot analysis showing increased ABCE1 level in HeLa cells transfected with NOT4-myc and treated with 20 μM CCCP. CCCP treatment further enhanced ABCE1 level in NOT4 transfected cells. * and < mark NOT4-myc and endogenous NOT4, respectively.

Figure S4. Additional Evidence Supporting Target Specificity of the siRNAs and Antibodies Used for the Co-translational Quality Control Factors and Data Showing the Effect of Inhibiting Co-translational Quality Control Factors on GFP-Parkin Recruitment to Mitochondria in HeLa/GFP-Parkin cells, Related to Figure 4

(A) Immunoblots showing knockdown of the expression of corresponding proteins by ABCE1, Pelo, and NOT4 siRNAs.

(B) Immunoblots showing detection of the corresponding tagged proteins expressed from the transfected cDNAs. * and < mark transfected and endogenous proteins, respectively.

(C) Immunoblots showing effect of knockdown of ABCE1, Pelo, and NOT4 protein by siRNAs on the recruitment of autophagy receptors to C-I30 mRNP purified from HeLa cells.

(D) Immunoblots showing that protein expression from the RNAi-resistant (rs) cDNA constructs is immune to the silencing effect of the respective siRNAs.

(E) Immunoblot showing the rescue of the ABCE1, Pelo, and NOT4 siRNA effects on p-TBK1 recruitment to *C-I30* mRNP by the corresponding rs cDNAs.

(F, G) Immunostainings showing rescue by rs cDNAs of the mitochondrial clearance defects caused by ABCE1, Pelo, and NOT4 siRNAs. Data quantification is shown in F. More than 200 cells were counted in the siRNA groups; while more than 50 positive cells were found and counted in the rsABCE1, rsPelo and rsNOT4 rescue groups.

(H) Immunostaining showing reduced Parkin recruitment to damaged mitochondria by ABCE1, Pelo, and NOT4 siRNAs. Data quantification is shown in Figure 3B.

Figure S5. Evidence Supporting PINK1-Dependent Poly-ubiquitination of ABCE1, and Effects of Mitochondrial Damage on ABCE1 Interaction with Pelo and NOT4, Related to Figure 5

(A) Immunoblots showing primarily K48-linked poly-ubiquitination on ABCE1 in CCCP treated cells.

(B, C) Immunoblots showing lack of direct interaction between Pelo and fly p62 (B) or between Pelo and mammalian autophagy receptors in HeLa/GFP-Parkin cells (C).

(D) Immunoblots showing that ABCE1 overexpression accelerated the recruitment of autophagy receptors to C-I30 mRNP associated with HeLa/GFP-Parkin cell mitochondria. > marks position of GFP-Parkin. (S) and (L) denote short and long exposures.

(E) Immunoblots showing the effect of overexpression of co-translational quality control factors on the association of fly p62 with ribosomal fractions prepared from muscle mitochondria.

(F) Immunoblot of denaturing IP showing the dependence of ABCE1 ubiquitination on PINK1.

(G) *In vitro* ubiquitination of ABCE1 by NOT4 using mutant forms of Ub. No-K, all K residues mutated to R; 48O, all but K48 mutated to R; 48R, only K48 mutated to R.

(H, I) Examining the effect of various E3 ligases on ABCE1 ubiquitination in fly muscle or HeLa cells. ABCE1 co-expressed with the various E3 ligases was IPed from fly muscle tissue (H) or transfected HeLa cells (I), and the extent of ABCE1 ubiquitination was assessed by western blot with anti-Ub.

(J) Immunoblots detecting levels of actin and C-I30 proteins in *PINK1(-/-)* mutant HeLa cells treated with graded concentrations of CCCP for the indicated periods.

(K) ATP measurement of *PINK1(-/-)* mutant HeLa cells treated with 20 μM CCCP for the indicated times. Relative ATP levels normalized to time 0 are used in statistical analysis. ** indicates $p<0.005$ in Student's *t*-test.

(L) Immunoblots of ABCE1 IP showing biphasic ABCE1-Pelo interaction in response to different durations of CCCP treatment, and persistent strengthening of ABCE1-NOT4 interaction and increase of poly-Ub-ABCE1 level in HeLa cells treated with 20 μM CCCP, and the absence of such molecular changes in *PINK1*(-/-) HeLa cells.

(M) Immunoblots showing the differential response of C-I75 and C-I30 protein levels to CCCP treatment in HeLa cells. The lack of change of Tom20 level indicates that the reduction of C-I30 level is not caused by mitophagy. * marks the precursor form of C-I75.

Figure S6. Additional *In vivo* Evidence Supporting the Involvement of Co-translational Quality Control Factors in PINK1-Directed Mitophagy, Related to Figure 6

(A-E) Effects of overexpression (OE) of co-translational quality control factors on muscle mitochondrial morphology (A), wing posture (B), ATP production (C), DA neuron mitochondria morphology (D), and DA neuron number (E) in wild type background expressing the mito-GFP reporter.

(F) Immunoblots showing the effect of co-translational quality control factor OE on C-I30 protein expression and LC3 II formation.

(G) Immunoblots showing blockage by ATG1 RNAi of the effect of co-translational quality control factor OE on C-I30 protein expression and LC3 II formation.

(H) Bar graph showing rescue of DA neuron loss in *PINK1* mutant by OE of co-translational quality control factors (*, $p<0.05$ in Student's *t*-test), and the blockage of such rescuing effects by ATG1 RNAi (#, $p<0.05$ in Student's *t*-test).

(I, J) Immunostaining of *PINK1(-/-)* mutant HeLa cells transfected with ABCE1 or co-transfected with ABCE1 and NOT4, and treated with or without 20 μM CCCP. Arrows mark the induction by ABCE1 and NOT4 of LC3-positive ring-like structures encircling mitochondria. Transfected ABCE1 is tagged with Flag. NOT4 and ABCE1 plasmids are transfected at 3:1 ratio such that all ABCE1-positive cells are most likely also NOT4-positive. Data quantification is shown in J. **, $p<0.005$ in *Chi-squared* test. Around 100 cells were counted in each group.

Figure S7. Analysis of Transcript Levels of Additional Genes in PD and Control Subject Brain Samples, Related to Figure 7

(A-C) Relative levels of mRNA expression in prefrontal cortex between PD cases and healthy control subjects for autophagy receptors (A), familial PD genes (B), and OxPhos related genes (C). None showed significant differential expression after multiple hypothesis correction. Note that although FBXO7 and UQCRC2 had nominal p-values < 0.05, neither had significant FDR.

Figure S1

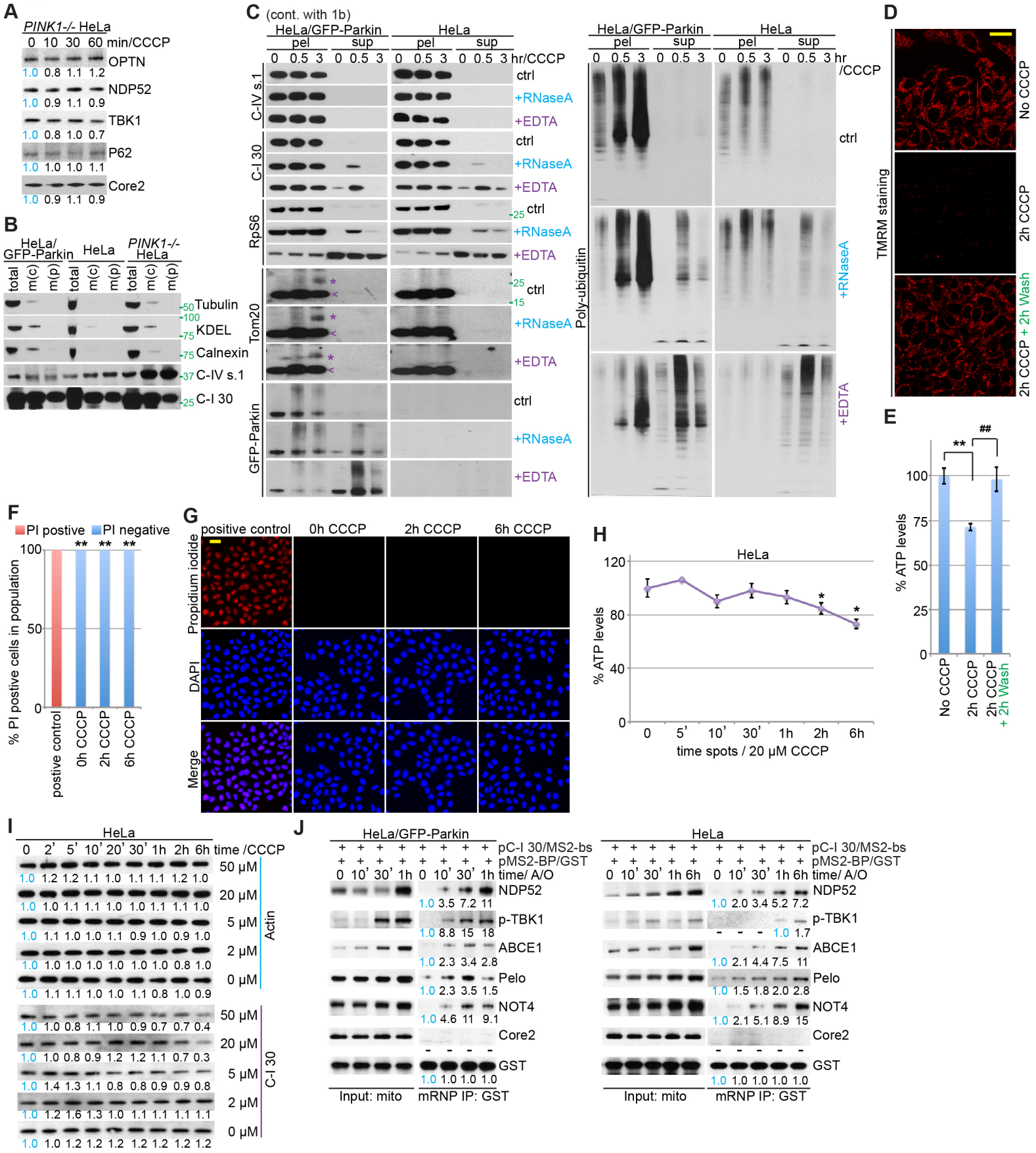
A
PINK1-/- HeLa
0 10 30 60 min/CCCP
OPTN
1.0 0.8 1.1 1.2
NDP52
1.0 0.9 1.1 0.9
TBK1
1.0 0.8 1.0 0.7
P62
1.0 1.0 1.0 1.1
Core2
1.0 0.9 1.1 0.9
B
HeLa/ GFP-Parkin
HeLa
PINK1-/- HeLa
total m(c) m(p) total m(c) m(p) total m(c) m(p)
Tubulin
KDEL
Calnexin
C-IV s.1
C-I 30
C (cont. with 1b)
HeLa/GFP-Parkin
HeLa
pel sup pel sup
0 0.5 3 0 0.5 3 0 0.5 3 0 0.5 3 hr/CCCP
C-IV s.1
C-I 30
RpS6
Tom20
GFP-Parkin
ctrl
+RNaseA
+EDTA
Poly-ubiquitin
D
TMRM staining
No CCCP
2h CCCP
2h CCCP + 2h Wash
E
% ATP levels
No CCCP
2h CCCP
2h CCCP + 2h Wash
F
PI postive
PI negative
% PI postive cells in population
postive control
0h CCCP
2h CCCP
6h CCCP
G
positive control
0h CCCP
2h CCCP
6h CCCP
Propidium iodide
DAPI
Merge
H
HeLa
% ATP levels
time spots / 20 μM CCCP
I
HeLa
0 2' 5' 10' 20' 30' 1h 2h 6h time /CCCP
50 μM
20 μM
5 μM
2 μM
0 μM
Actin
C-I 30
J
HeLa/GFP-Parkin
HeLa
pC-I 30/MS2-bs
pMS2-BP/GST
time/ A/O
NDP52
p-TBK1
ABCE1
Pelo
NOT4
Core2
GST
Input: mito
mRNP IP: GST

Figure S2

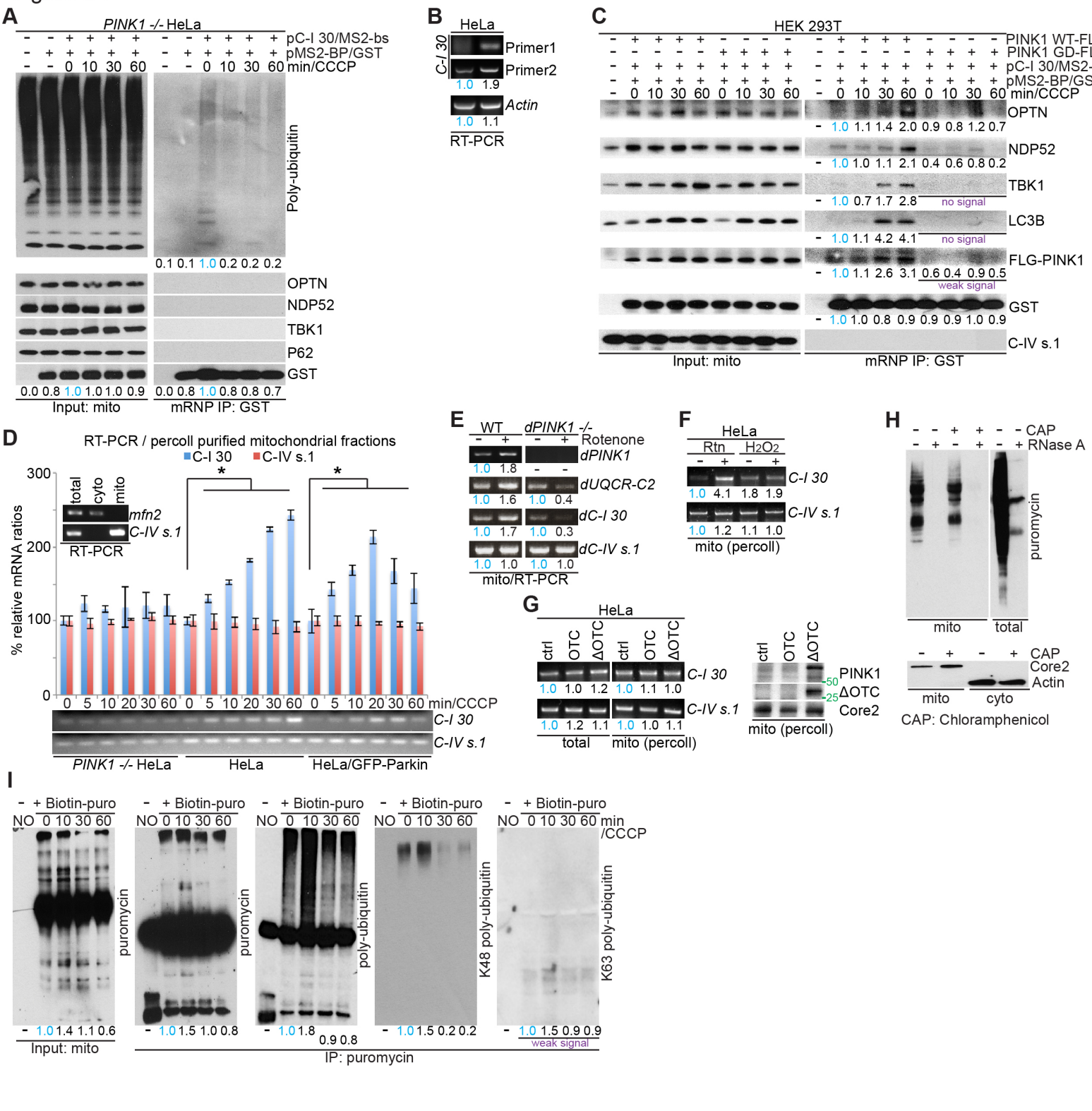
A
PINK1 -/- HeLa
pC-I 30/MS2-bs
pMS2-BP/GST
min/CCCP
Poly-ubiquitin
OPTN
NDP52
TBK1
P62
GST
Input: mito
mRNP IP: GST
B
HeLa
C-I 30
Primer1
Primer2
Actin
RT-PCR
C
HEK 293T
PINK1 WT-FLG
PINK1 GD-FLG
pC-I 30/MS2-bs
pMS2-BP/GST
min/CCCP
OPTN
NDP52
TBK1
LC3B
FLG-PINK1
GST
C-IV s.1
no signal
weak signal
Input: mito
mRNP IP: GST
D
RT-PCR / percoll purified mitochondrial fractions
C-I 30
C-IV s.1
% relative mRNA ratios
total
cyto
mito
mfn2
C-IV s.1
RT-PCR
min/CCCP
C-I 30
C-IV s.1
PINK1 -/- HeLa
HeLa
HeLa/GFP-Parkin
E
WT
dPINK1 -/-
Rotenone
dPINK1
dUQCR-C2
dC-I 30
dC-IV s.1
mito/RT-PCR
F
HeLa
Rtn
H2O2
C-I 30
C-IV s.1
mito (percoll)
G
HeLa
ctrl
OTC
ΔOTC
C-I 30
C-IV s.1
total
mito (percoll)
PINK1
ΔOTC
Core2
H
CAP
RNase A
puromycin
mito
total
Core2
Actin
cyto
CAP: Chloramphenicol
I
+ Biotin-puro
NO
min
/CCCP
puromycin
poly-ubiquitin
K48 poly-ubiquitin
K63 poly-ubiquitin
Input: mito
IP: puromycin
weak signal

Figure S3

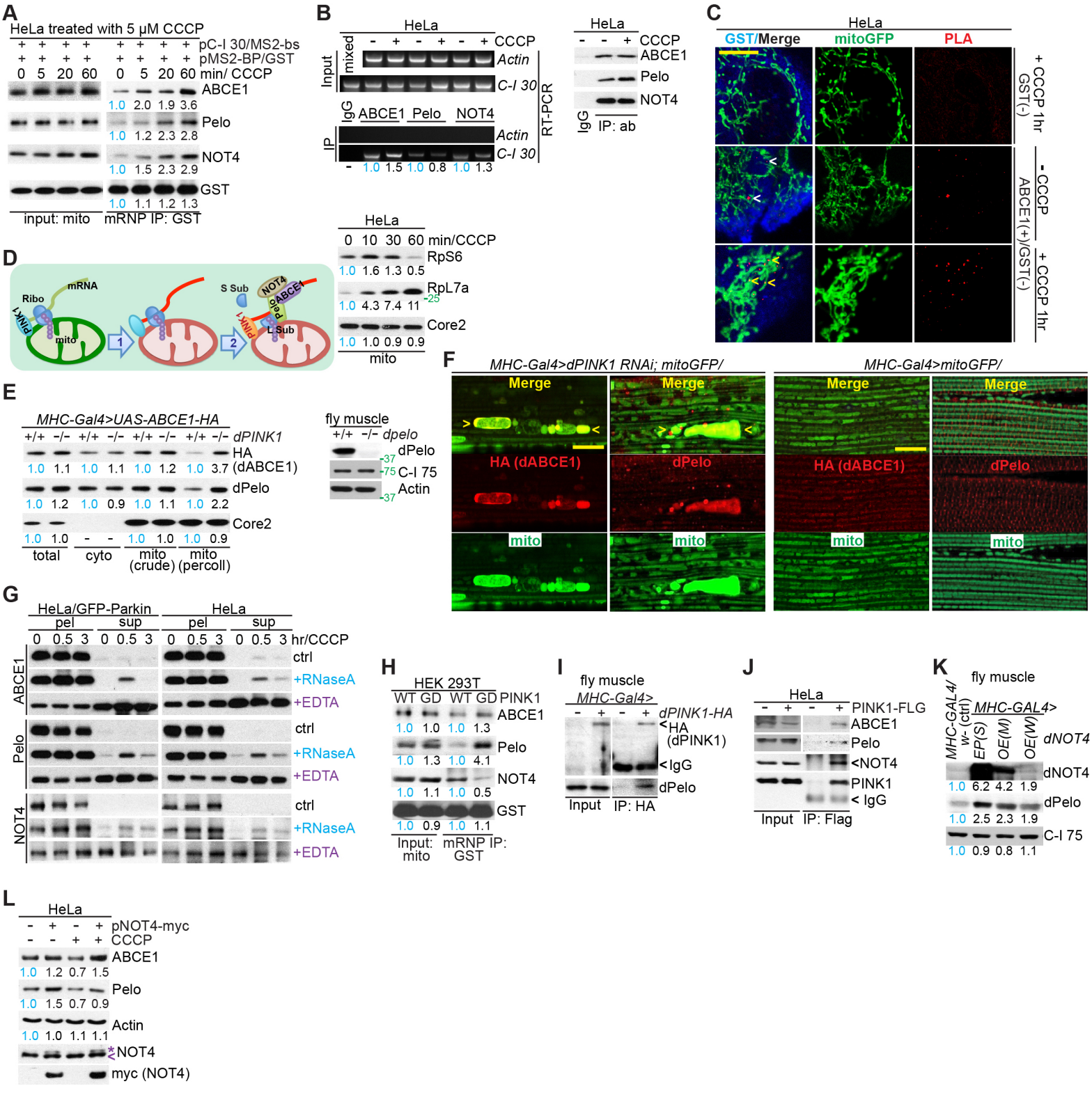
A
HeLa treated with 5 μM CCCP
pC-I 30/MS2-bs
pMS2-BP/GST
0 5 20 60 0 5 20 60 min/ CCCP
ABCE1
1.0 2.0 1.9 3.6
Pelo
1.0 1.2 2.3 2.8
NOT4
1.0 1.5 2.3 2.9
GST
1.0 1.1 1.2 1.3
input: mito
mRNP IP: GST
B
HeLa
CCCP
Input
mixed
Actin
C-I 30
RT-PCR
IgG ABCE1 Pelo NOT4
IP
Actin
C-I 30
1.0 1.5 1.0 0.8 1.0 1.3
HeLa
CCCP
ABCE1
Pelo
NOT4
IgG
IP: ab
HeLa
0 10 30 60 min/CCCP
RpS6
1.0 1.6 1.3 0.5
RpL7a
1.0 4.3 7.4 11
Core2
1.0 1.0 0.9 0.9
mito
C
HeLa
GST/Merge
mitoGFP
PLA
+ CCCP 1hr GST(-)
- CCCP ABCE1(+)/GST(-)
+ CCCP 1hr
D
Ribo
mRNA
PINK1
mito
1
S Sub
NOT4
ABCE1
Pelo
PINK1
L Sub
2
E
MHC-Gal4>UAS-ABCE1-HA
+/+ -/- +/+ -/- +/+ -/- +/+ -/- dPINK1
HA
1.0 1.1 1.0 1.1 1.0 1.2 1.0 3.7 (dABCE1)
dPelo
1.0 1.2 1.0 0.9 1.0 1.1 1.0 2.2
Core2
1.0 1.0 - - 1.0 1.0 1.0 0.9
total
cyto
mito (crude)
mito (percoll)
fly muscle
+/+ -/- dpelo
dPelo
-37
-75
C-I 75
Actin
-37
F
MHC-Gal4>dPINK1 RNAi; mitoGFP/
MHC-Gal4>mitoGFP/
Merge
HA (dABCE1)
dPelo
mito
G
HeLa/GFP-Parkin
HeLa
pel sup pel sup
0 0.5 3 0 0.5 3 0 0.5 3 0 0.5 3 hr/CCCP
ABCE1
Pelo
NOT4
ctrl
+RNaseA
+EDTA
H
HEK 293T
WT GD WT GD PINK1
ABCE1
1.0 1.0 1.0 1.3
Pelo
1.0 1.3 1.0 4.1
NOT4
1.0 1.1 1.0 0.5
GST
1.0 0.9 1.0 1.1
Input: mito
mRNP IP: GST
I
fly muscle
MHC-Gal4>
dPINK1-HA
HA (dPINK1)
IgG
dPelo
Input
IP: HA
J
HeLa
PINK1-FLG
ABCE1
Pelo
NOT4
PINK1
IgG
Input
IP: Flag
K
fly muscle
MHC-GAL4/ w- (ctrl)
MHC-GAL4>
EP(S)
OE(M)
OE(W)
dNOT4
dNOT4
1.0 6.2 4.2 1.9
dPelo
1.0 2.5 2.3 1.9
C-I 75
1.0 0.9 0.8 1.1
L
HeLa
pNOT4-myc
CCCP
ABCE1
1.0 1.2 0.7 1.5
Pelo
1.0 1.5 0.7 0.9
Actin
1.0 1.0 1.1 1.1
NOT4
myc (NOT4)

Figure S4

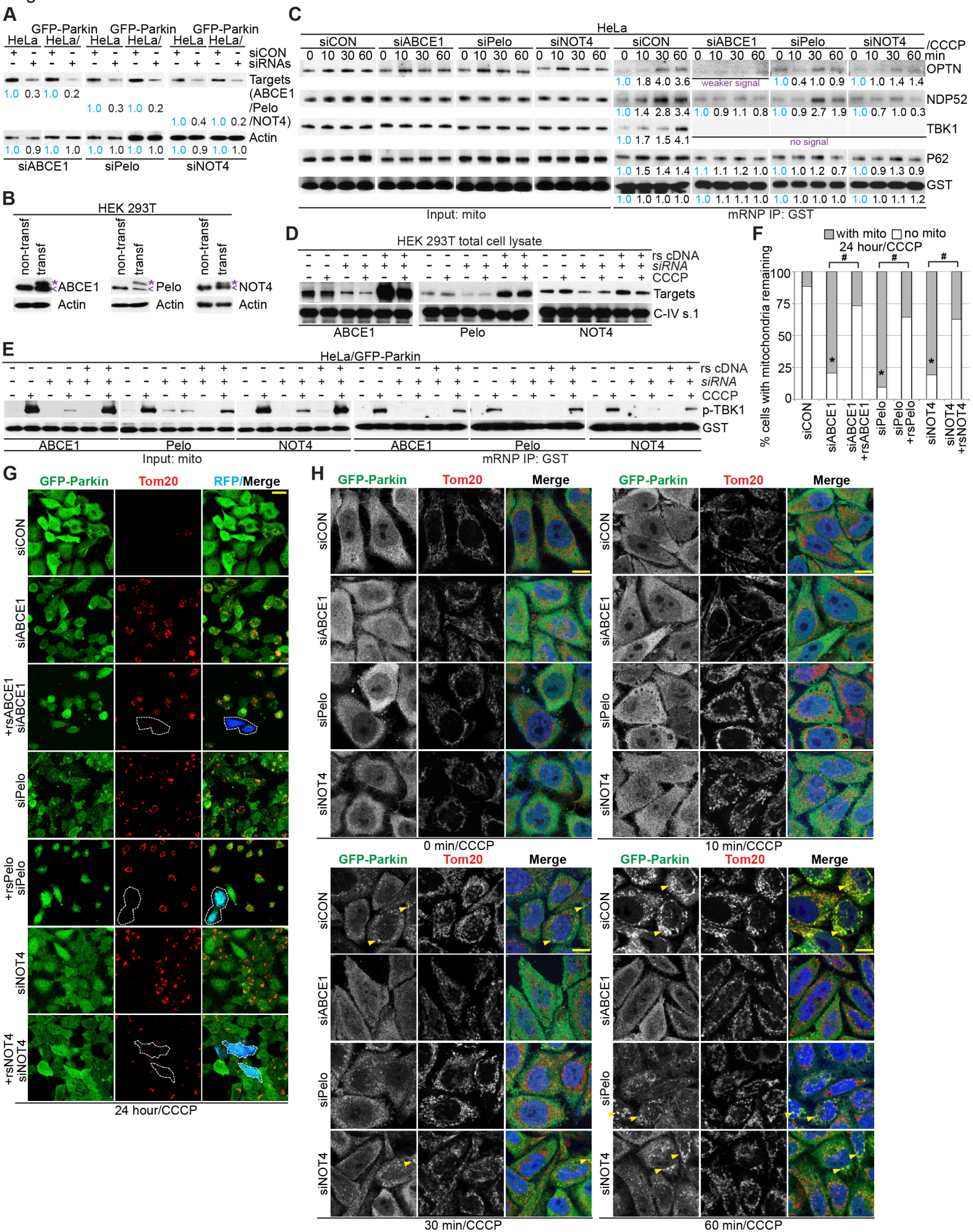
A
GFP-Parkin
HeLa
HeLa/
siCON
siRNAs
Targets (ABCE1 /Pelo /NOT4)
Actin
siABCE1
siPelo
siNOT4
B
HEK 293T
non-transf
transf
ABCE1
Pelo
NOT4
Actin
C
HeLa
siCON
siABCE1
siPelo
siNOT4
/CCCP
min
OPTN
NDP52
TBK1
P62
GST
weaker signal
no signal
Input: mito
mRNP IP: GST
D
HEK 293T total cell lysate
rs cDNA
siRNA
CCCP
Targets
C-IV s.1
ABCE1
Pelo
NOT4
E
HeLa/GFP-Parkin
rs cDNA
siRNA
CCCP
p-TBK1
GST
ABCE1
Pelo
NOT4
Input: mito
mRNP IP: GST
F
with mito
no mito
24 hour/CCCP
% cells with mitochondria remaining
siCON
siABCE1
siABCE1 +rsABCE1
siPelo
siPelo +rsPelo
siNOT4
siNOT4 +rsNOT4
G
GFP-Parkin
Tom20
RFP/Merge
siCON
siABCE1
+rsABCE1 siABCE1
siPelo
+rsPelo siPelo
siNOT4
+rsNOT4 siNOT4
24 hour/CCCP
H
GFP-Parkin
Tom20
Merge
0 min/CCCP
10 min/CCCP
30 min/CCCP
60 min/CCCP

Figure S5

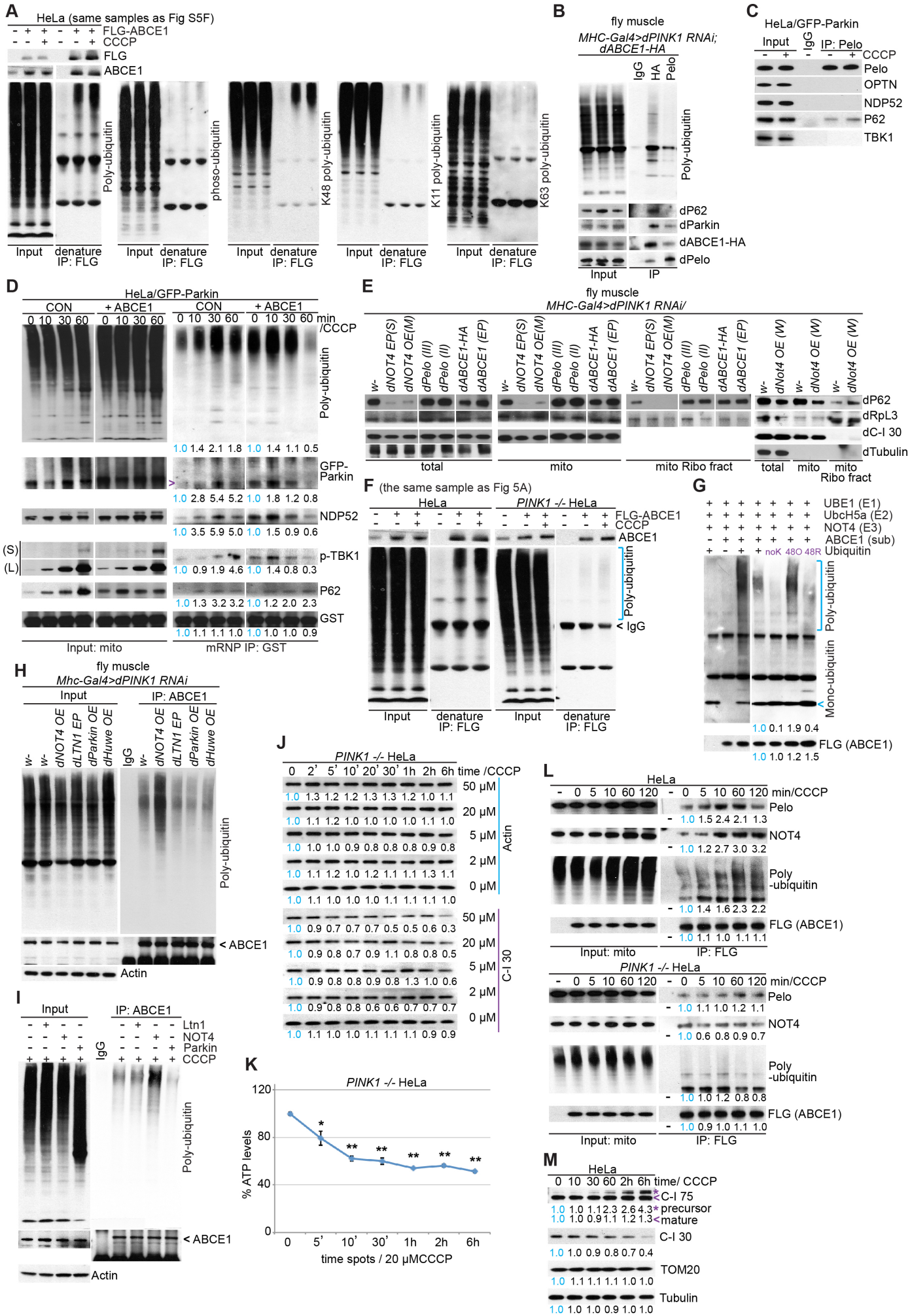
A
HeLa (same samples as Fig S5F)
FLG-ABCE1
CCCP
FLG
ABCE1
Poly-ubiquitin
phoso-ubiquitin
K48 poly-ubiquitin
K11 poly-ubiquitin
K63 poly-ubiquitin
Input
denature IP: FLG
B
fly muscle
MHC-Gal4>dPINK1 RNAi; dABCE1-HA
IgG
HA
Pelo
Poly-ubiquitin
dP62
dParkin
dABCE1-HA
dPelo
Input
IP
C
HeLa/GFP-Parkin
Input
IgG
IP: Pelo
CCCP
Pelo
OPTN
NDP52
P62
TBK1
D
HeLa/GFP-Parkin
CON
+ ABCE1
0 10 30 60 min /CCCP
Poly-ubiquitin
GFP-Parkin
NDP52
p-TBK1
(S)
(L)
P62
GST
Input: mito
mRNP IP: GST
E
fly muscle
MHC-Gal4>dPINK1 RNAi/
w-
dNOT4 EP(S)
dNOT4 OE(M)
dPelo (III)
dPelo (II)
dABCE1-HA
dABCE1 (EP)
dNot4 OE (W)
dP62
dRpL3
dC-I 30
dTubulin
total
mito
mito Ribo fract
F
(the same sample as Fig 5A)
HeLa
PINK1 -/- HeLa
FLG-ABCE1
CCCP
ABCE1
Poly-ubiquitin
IgG
Input
denature IP: FLG
G
UBE1 (E1)
UbcH5a (E2)
NOT4 (E3)
ABCE1 (sub)
Ubiquitin
noK
48O
48R
Poly-ubiquitin
Mono-ubiquitin
FLG (ABCE1)
H
fly muscle
Mhc-Gal4>dPINK1 RNAi
Input
IP: ABCE1
w-
dNOT4 OE
dLTN1 EP
dParkin OE
dHuwe OE
IgG
Poly-ubiquitin
ABCE1
Actin
I
Input
IP: ABCE1
Ltn1
NOT4
Parkin
CCCP
IgG
Poly-ubiquitin
ABCE1
Actin
J
PINK1 -/- HeLa
0 2' 5' 10' 20' 30' 1h 2h 6h time /CCCP
50 μM
20 μM
5 μM
2 μM
0 μM
Actin
C-I 30
K
PINK1 -/- HeLa
% ATP levels
time spots / 20 μMCCCP
L
HeLa
min/CCCP
Pelo
NOT4
Poly -ubiquitin
FLG (ABCE1)
Input: mito
IP: FLG
PINK1 -/- HeLa
M
HeLa
0 10 30 60 2h 6h time/ CCCP
C-I 75
precursor
mature
C-I 30
TOM20
Tubulin

Figure S6

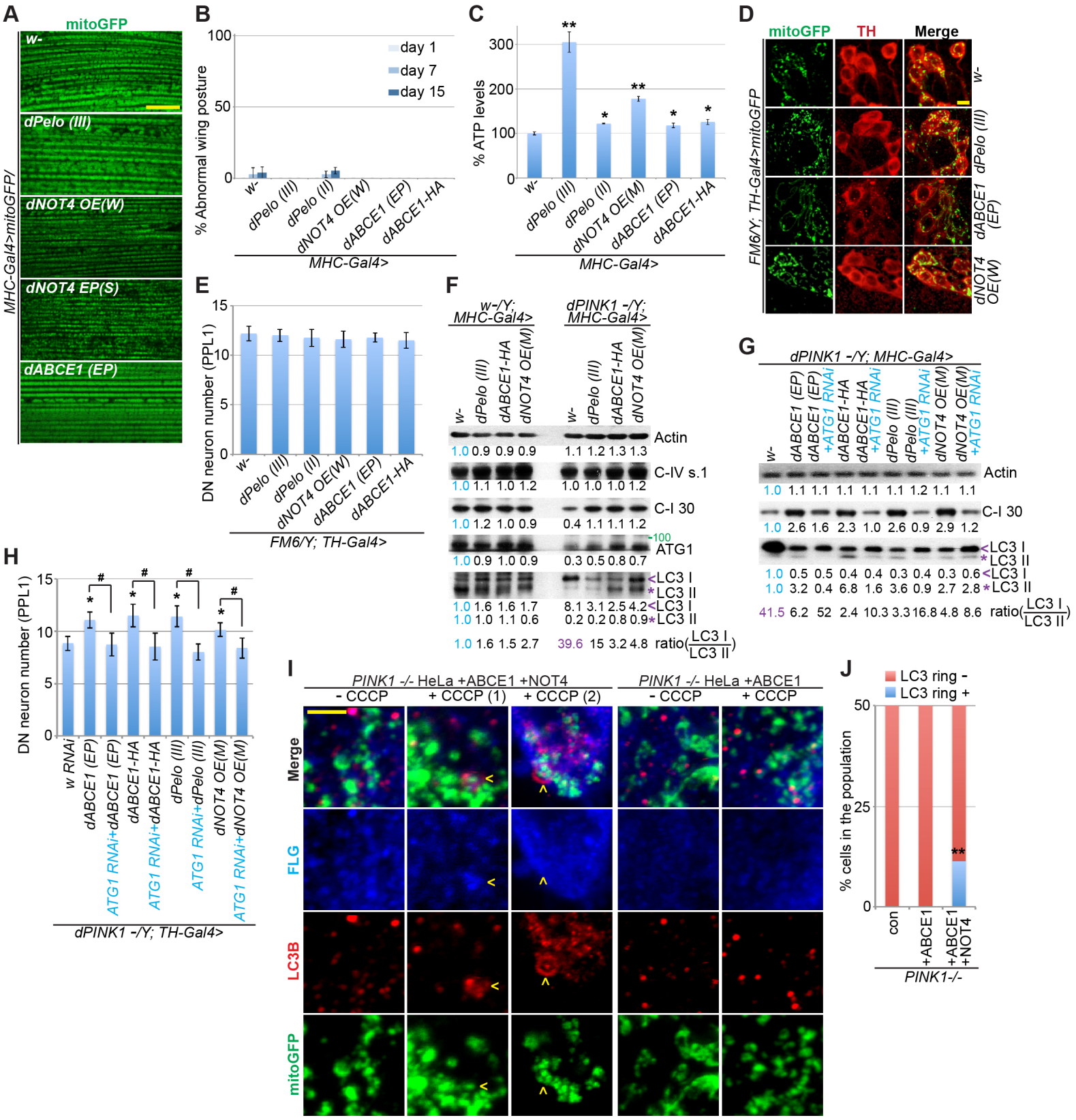
A
mitoGFP
w-
dPelo (III)
dNOT4 OE(W)
dNOT4 EP(S)
dABCE1 (EP)
MHC-Gal4>mitoGFP/
B
% Abnormal wing posture
day 1
day 7
day 15
w-
dPelo (III)
dPelo (II)
dNOT4 OE(W)
dABCE1 (EP)
dABCE1-HA
MHC-Gal4>
C
% ATP levels
MHC-Gal4>
D
mitoGFP
TH
Merge
FM6/Y; TH-Gal4>mitoGFP
dABCE1 (EP)
dNOT4 OE(W)
E
DN neuron number (PPL1)
FM6/Y; TH-Gal4>
F
w-/Y; MHC-Gal4>
dPINK1 -/Y; MHC-Gal4>
Actin
C-IV s.1
C-I 30
ATG1
LC3 I
LC3 II
ratio(LC3 I / LC3 II)
G
dPINK1 -/Y; MHC-Gal4>
dABCE1 (EP)
+ATG1 RNAi
dABCE1-HA
dPelo (III)
dNOT4 OE(M)
Actin
C-I 30
LC3 I
LC3 II
ratio(LC3 I / LC3 II)
H
DN neuron number (PPL1)
w RNAi
dABCE1 (EP)
ATG1 RNAi+dABCE1 (EP)
dABCE1-HA
ATG1 RNAi+dABCE1-HA
dPelo (III)
ATG1 RNAi+dPelo (III)
dNOT4 OE(M)
ATG1 RNAi+dNOT4 OE(M)
dPINK1 -/Y; TH-Gal4>
I
PINK1 -/- HeLa +ABCE1 +NOT4
- CCCP
+ CCCP (1)
+ CCCP (2)
PINK1 -/- HeLa +ABCE1
- CCCP
+ CCCP
Merge
FLG
LC3B
mitoGFP
J
LC3 ring -
LC3 ring +
% cells in the population
con
+ABCE1
+ABCE1 +NOT4
PINK1-/-

Figure S7

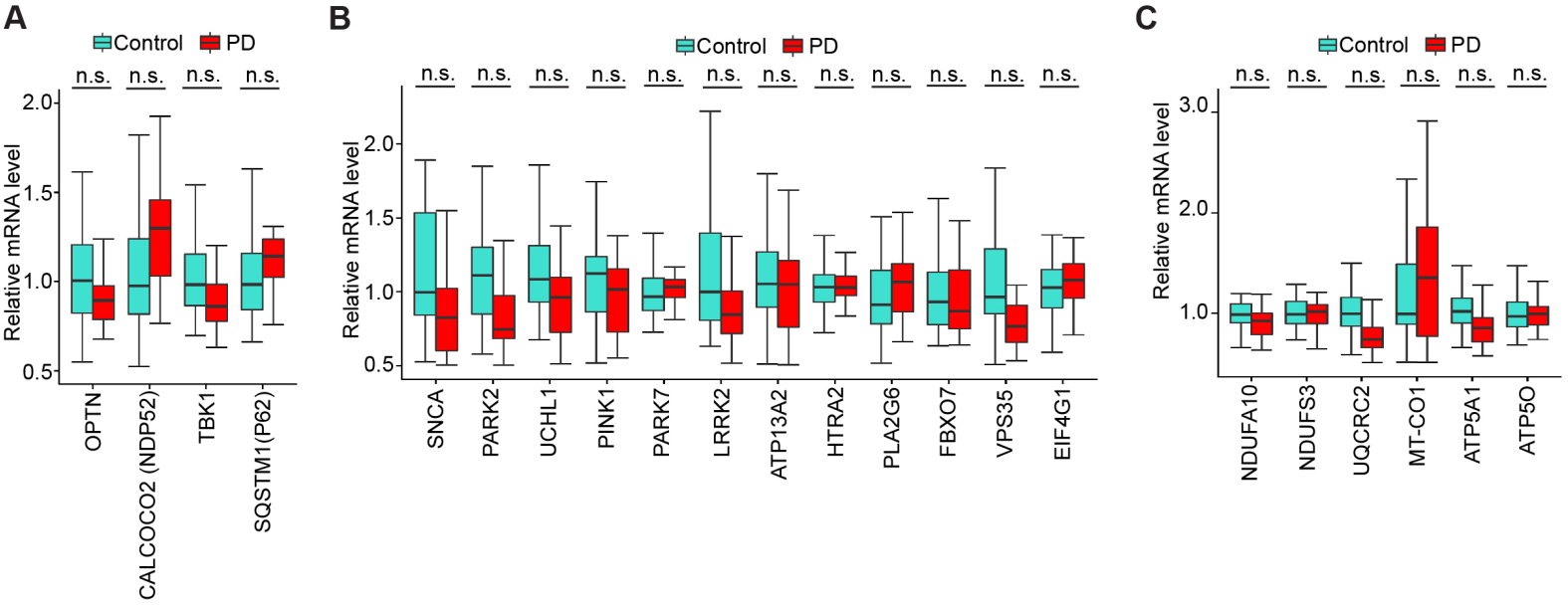
A
Control
PD
n.s.
Relative mRNA level
2.0
1.5
1.0
0.5
OPTN
CALCOCO2 (NDP52)
TBK1
SQSTM1(P62)
B
SNCA
PARK2
UCHL1
PINK1
PARK7
LRRK2
ATP13A2
HTRA2
PLA2G6
FBXO7
VPS35
EIF4G1
C
3.0
NDUFA10
NDUFS3
UQCRC2
MT-CO1
ATP5A1
ATP5O